VISUALIZATION OF ICE SLURRIES AND ICE SLURRY FLOWS

O. SARI, D. VUARNOZ, F. MEILI
University of Applied Sciences of Western Switzerland
CH-1401 Yverdon-les-Bains, Switzerland

P. W. EGOLF
Swiss Federal Laboratories for Materials Testing and Research
CH-8600 Dübendorf, Switzerland

Visualizations of ice particles in a rectangular cavity and ice slurry flows in a pipe are performed. The form and size of ice particles is investigated by optical microscopy. It permits to evaluate statistically the geometrical shapes of the ice crystals. The observed particle densities and the size distributions correspond with the theoretically determined ice fractions. - A method applied to measure ice slurry velocity fields is based on ultrasound Doppler echography. The velocity profile, determined by the velocity of ice particles, is measured and several features which are related to Bingham flows are observed. With these experimental results complete rheograms can be constructed.

1. INTRODUCTION

Ice slurry research has its origin in the domain of refrigeration technology. Therefore, most investigations were directed to systems and related problems. Up till now much less effort has been undertaken to solve basic physical and chemical problems. But the number of such investigations is now increasing rapidly. This is important, because an optimization of ice slurry systems is only possible, when basic physical knowledge is available. For example the relations between ice crystal sizes and shapes (see Ref.[1]) and the corresponding viscosities must be known. Or the mechanisms for the observed time behavior [2]. A further example is the knowledge of phase diagrams, e.g. giving informations on the occurring flow regimes (e.g. homogenous flow, heterogenous flow, saltation flow or flow with a stationary bed) as a function of the parameters of the forced rheological system under consideration [3].

Particle shape and size analysis is a large field of elementary particle and solid state physics, chemistry, pharmaceutics, biology, etc. Therefore, a large number of techniques have been developed, e.g. sedimentation and sieving, microscopy, numerous light scattering methods, laser light diffraction techniques, etc. (for an overview see e.g. Ref. [4] and [5]). Because of the rather large size of the ice particles in the ice slurries (30μm-300μm), an ordinary light microscopic method is applied. The disadvantage of this technique are the two-dimensional projections obtained of the particles, which show irregular shapes. Microscopic pictures of ice slurry particles were also published, e.g. by Fukusako et al. [6], Bel [7] and Kauffeld et al. [8]. Independently of the applied additives in each case the ice crystals show approximately ellipsoidal shapes. This is also confirmed by the work presented in this article. Furthermore, the intention of the present study was to statistically evaluate ensembles of ice particles.

The second objective was to gain some knowledge on the intrinsic flow of ice slurries. Ultra sound echography is applied. This method, based on the Doppler effect, has been widely used to investigate a number of specific rheological flows. The measuring technique is applied for numerous scientific purposes (e.g. Ref. [9] to [11]) as well as to perform industrial quality control [12]. Kawashima et al. studied ice slurry flows (snow water mixtures) with a high-speed video camera [13].

2. EXPERIMENTAL SET-UP

The ice slurry installation used as basis for all the presented visualization experiments is described in [14] and shown in figure 1. The talin mass fraction in the ice slurries produced was always 11 %.

The shape and size of the ice crystals depend on the temperature of the suspension and several further system parameters, quantified in chapter 4.1. An overview is the following:

In the ice generator the creation of the ice crystals is influenced by:
- the rotation speed of the scraper
- the evaporation temperature of the refrigerant fluid
- the difference between the evaporation temperature and the temperature of the ice slurry
- the distance between the scraper and the cooling wall in the condensing unit.

In the storage tank:
- the rotation speed of the mixer
- the mean time of rest of the ice particles in the tank (time behaviour)
- if the mixing process is not ideal, the position of the outlet to the secondary circuit

In the piping system:
- the velocity of the fluid
- the heat transfer depending on insulation, etc.

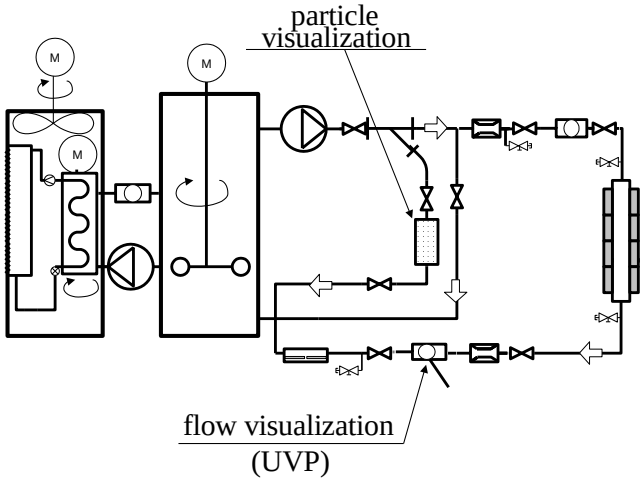

Figure 1: The experimental ice slurry testing system “Coulis” is shown. From the left to the right the ice generator, the storage tank, the visualization circuit with the measuring devices and a cylindrical heat exchanger (used to perform the work presented in [18]) can be seen.

3. MEASURING TECHNIQUES

3.1 Microscopy

The microscopic instrument applied produces pictures by diffraction with a diascopic method. The wave length of the halogen light is approximately 300-700 μm. To take black and white pictures on the microscope a CCD camera is mounted (figure 2). The microscope and camera are focussed to take pictures between the glass plates. The particles are transported from a location in the secondary circuit downstream of the pump to the observation chamber. For a photographic exposure the fluid was stopped for a very short time in the detection domain, bounded by two plexiglass plates of 2 mm distance. For each ensemble ten photographies were taken and this yields the material for the statistical evaluations.

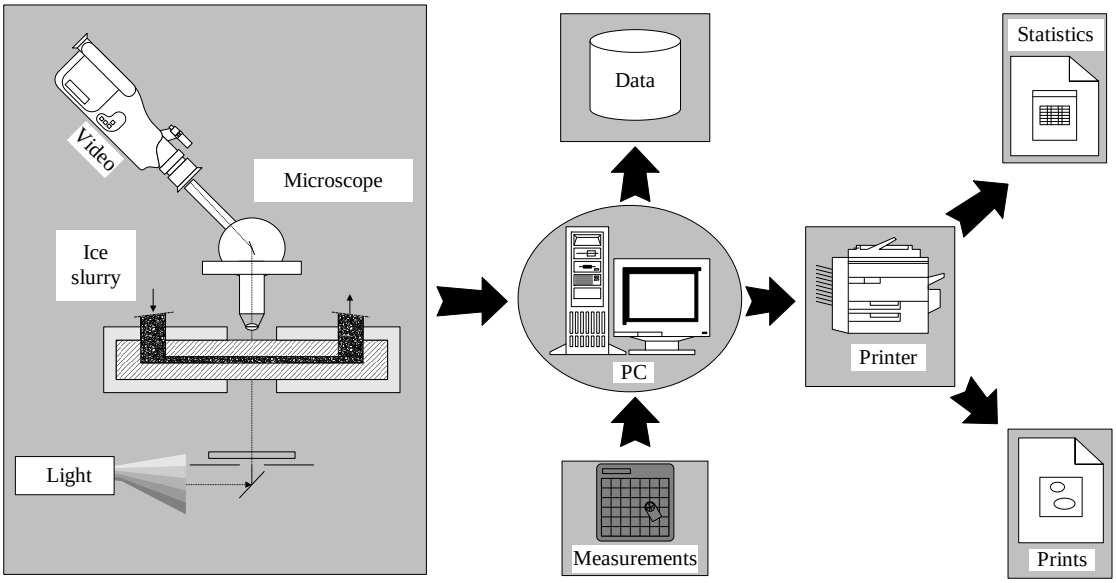

Figure 2: The entire infrastructure to evaluate statistical data on ice particles consists of a microscope, a digital camera and some other standard material.

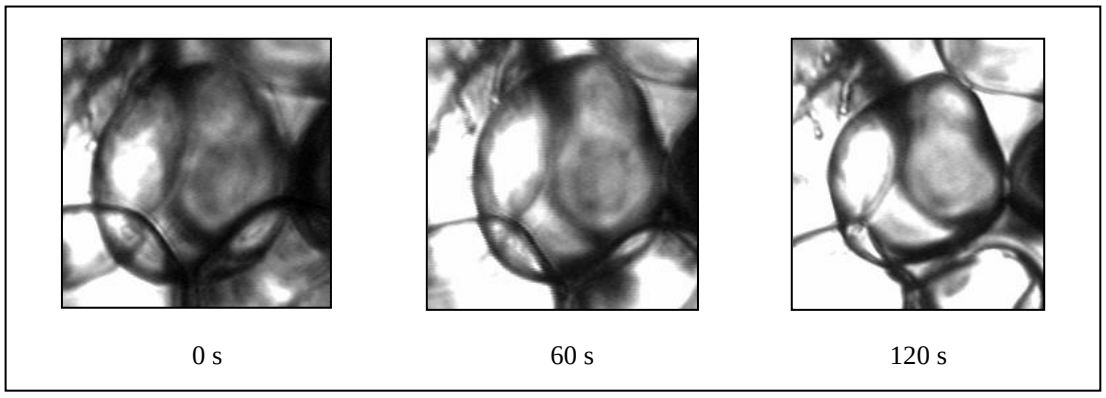

Figure 3: Three microscopic pictures taken at times 0 s, 60 s and 120 s. Clearly a shrinking of the focussed ice particle can be observed. At the contact positions with other ice particles melting is supressed. As a consequence the convexity of the particles locally alters.

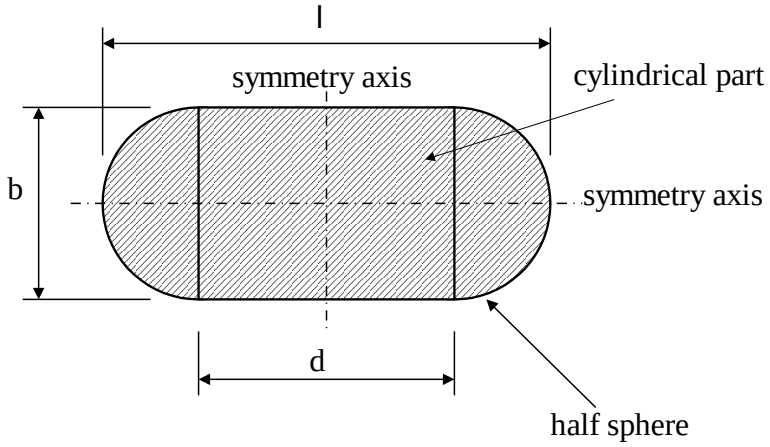

Figure 4: In a simple model the ice particles are approximated by small slabs with two half spheres on each side.

The aim is to achieve a high quality of the pictures. But this usually leads to a high energy input into the fluid. This effect produces a melting of the particles and, therefore, it must be avoided. Stopping the flow and taking a photograph takes five seconds. In figure 3 three photographs of an ice particle - taken in one minute intervals – are shown. The pictures allow an estimate of the thermal quality of the measuring device influenced by heat transfer from the environment. When two minutes passed by, the length of the observed particle decreased from 52.3 μm to 46.3 μm and the width reduced nearly the same amount, namely 5.9 μm.

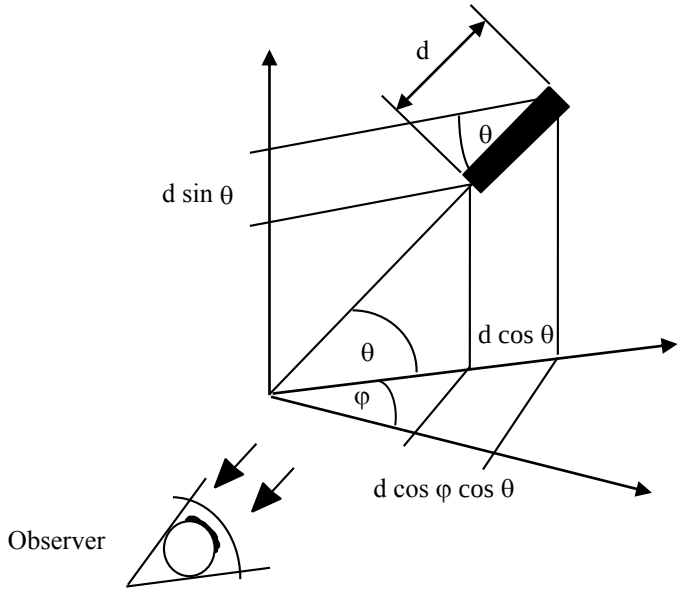

Figure 5: The 3-dimensional problem is characterized by the two angles of rotation φ and θ.

In the projection the ice particles approximately yield ellipses. The lengths of the two axes were measured exactly. As shown in figure 4 the larger axis has the length *"l"* and the smaller one the width *"b*". The ratio *l/b* is a measure for the excentricity of the particles.

Assuming that in the quiescent fluid the particles are distributed in a homogenous and isotropic manner, from the observed length d_{obs} (projection to a plane), it is possible to calculate the effective length *d* (see figure 5). An advantage of the applied model is that the width *b* does not alter in a projection. Symmetries are taken into consideration and, therefore, averages are calculated only of one eigth of the sphere. Then in spherical coordinates it follows that

$$\frac{\bar{d}_{obs}}{\bar{d}} = \frac{4}{\pi^2} I, \qquad I = \int_0^{\frac{\pi}{2}} \int_0^{\frac{\pi}{2}} \sqrt{\cos^2\varphi \cos^2\theta + \sin^2\theta}\; d\theta\; d\varphi \quad \Rightarrow \quad \bar{d} = \frac{\pi^2}{4} \frac{1}{I} \bar{d}_{obs} \qquad \text{(1a-c)}$$

A numerical calculation of the double integral leads to *I*=2.078. The effective mean length is 19 % larger than the mean of a large number of observed (projected) lengths. This factor is taken into consideration to apply a correction to the two-dimensional observation to approximate three-dimensional reality. Obviously, with the microscopic method some information on the specific solid distribution of particles is lost. The factor f = 1/1.19 = 0.84 is named view factor.

3.2 Ultra Sound Velocity Profile Meter

To analyze a flow the velocity profile is of fundamental importance. For example it permits to decide, if the regime is laminar or turbulent or if a fluid is Newtonian or shows a particular rheological behaviour. In the middle of the 80's at the Paul Scherrer institute (PSI) in Switzerland a special equipment, named ultrasonic velocity profiler (UVP) - based on the ultrasonic Doppler effect - was developed, which initially had been built for the medical domain. It was applied to different industrial flows and insiders founded a company, which now produces UVP measuring equipment.

Figure 6 helps to explain the principle of measurement. Laminar flows through a plexiglass pipe are studied. On the pipe an UVP transducer is mounted. The sensor emits an ultrasonic beam with a frequency of 2.0 MHz. On their path through the fluid the sound waves are attenuated. The particles reflect the waves and generate an echo. The reflected waves, which show a modified frequency - depending on the particle velocity - are detected by the transducer. With the Doppler principle the difference of the frequencies of the transmitted and reflected waves can be directly transformed to yield the particle velocity. The produced ultra sound wave beam has a diameter of 10 mm. Caused by this a measuring point can be related to a cylinder with this diameter and a height of 0.74 mm (see figure). Every measuring record is obtained as an average of an ensemble of 1028 velocity measurements determined at one space position. Several such records result in the averaged velocity profile. In the measurements the assumption is made that the direction of the velocity vector is parallel to the axis of the tube. Horizontal profiles through the center line of the pipe are determined.

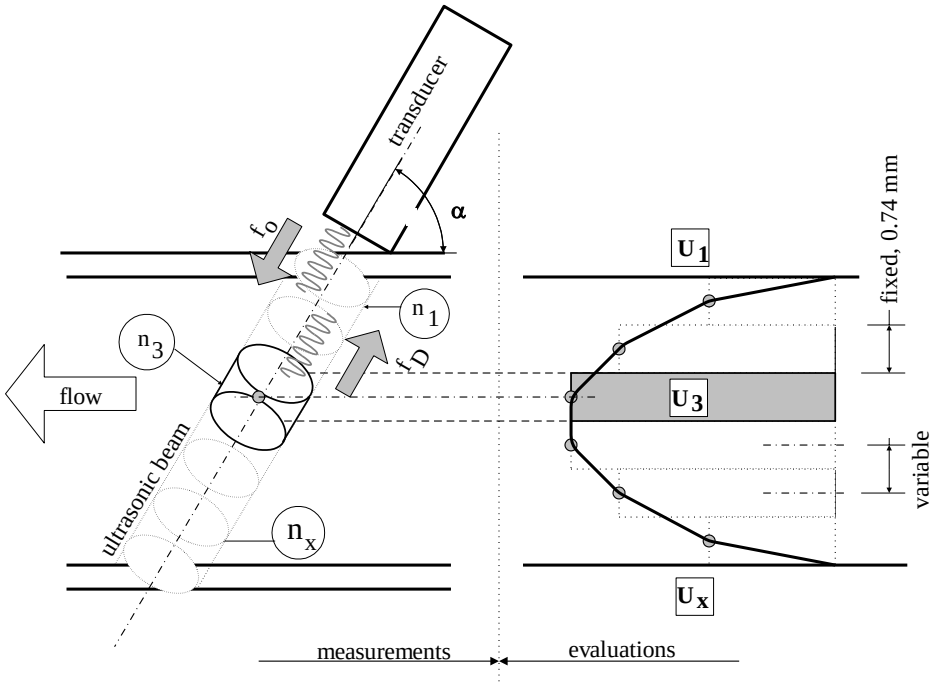

Figure 6: Schematic presentation of the velocity measurement principle by UVP on a horizontal ice slurry pipe. The number of chosen measuring positions (center of an ultrasonic beam) defines, together with further parameters, the quality of the obtained results. In the performed experiments a maximum of 128 measuring points are achieved.

4. EXPERIMENTAL RESULTS

4.1 Adjusted Parameters

The parameters of the installation chosen to obtain the presented results are:

- Mass fraction of talin c_T = 11%
- Mass fraction of ice c_I = 16 %
- Evaporation temperature T_{evap} = -13 °C
- Frequency of mixing element in the storage tank $n_{rot\ stock}$ = 236 min^{-1}
- Frequency of scraper in the ice generator $n_{rot\ prod}$ = 164 min^{-1}
- Mean temperature of the ice slurry ϑ = -5.7 °C.

4.2 Microscopy

The photographs show that in the quiescent fluid the solid ice particles are randomly distributed in the carrier fluid (see figure 7). Furthermore, it can be seen that the shape is approximately ellipsoidal, so that our ideas to model the particles should lead to useful results.

Bel classifies the ice crystals to have a hexagonal structure [7]. It could be that the geometry of the ice crystals as a consequence of collisions becomes a little smoother (rounder) as they are transported in the fluid. The particles may also undergo some metamorphoses [19]. Such mechanisms may explain the time behaviour observed by Frei et al. in their pressure drop measurements [2].

Numerous photographs have been statistically evaluated. The results of these investigations are shown in figure 7 and some statistical quantities are summarized in table 1.

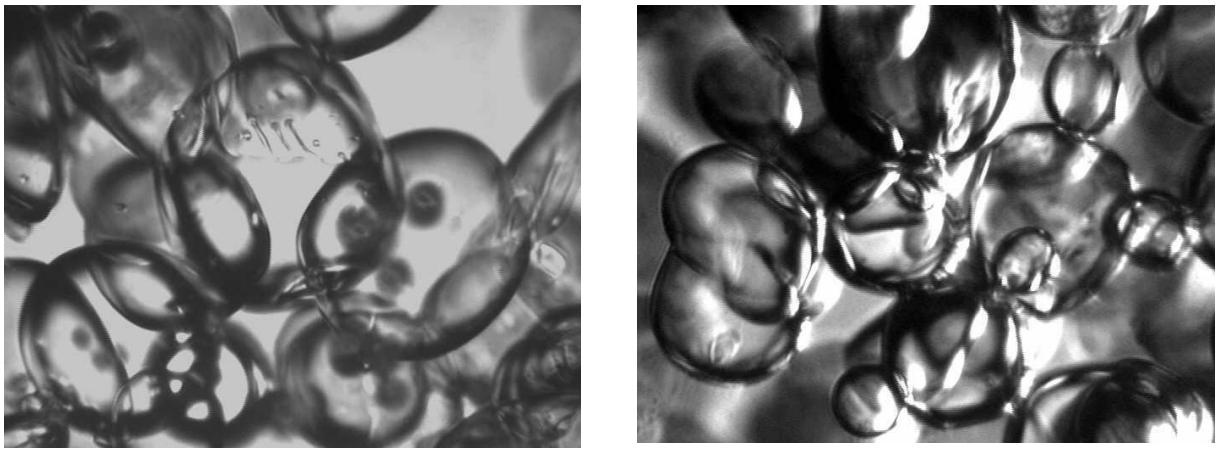

Figure 7: Two microscopic photographs with approximately fifteen particles each. The dimensions of the pictures are 1061 μm x 762 μm. On the left hand side an example of ensemble A, on the right hand side one of ensemble B are shown (for a definition of the ensembles see below).

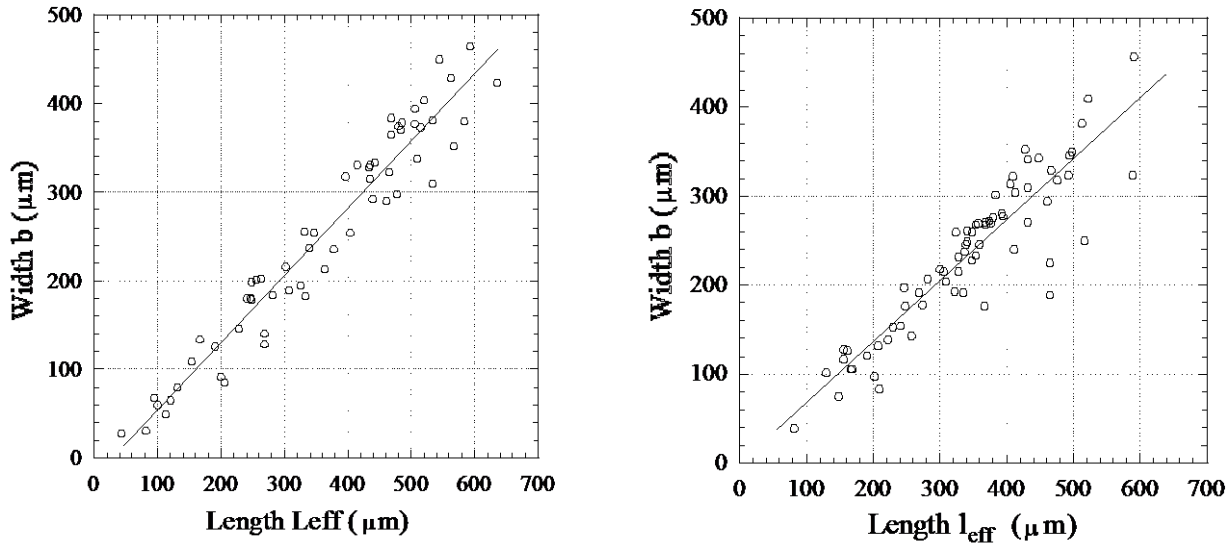

Figure 8: Informations on the corrected length l_{eff} and the width b of the observed ice particles. The figure on the left corresponds to ensemble A, the one on the right to ensemble B (see table 1).

A	Name	B
60	N	70
358	$<l>_{eff}$ (μm)	344
181	$\sigma_{l\,eff}$ (μm)	136
250	$<b>$ (μm)	234
119	σ_b (μm)	85
0.7	Length Ratio	0.68

Table 1 : Results of statistical evaluation. Two different ensembles have been observed in ten photographs each. The results of ensemble A are shown on the left, those of ensemble B on the right. *N* is the number of particles. For the other quantities see in the nomenclature.

The photographs of ensemble A and ensemble B have been taken in different experiments at different times. The time between the creation of the ice particles and the photographic exposure differs in the two experiments. The determined difference between the mean values of ensemble A and ensemble B is according to statistical laws to 99 % not significant. Therefore, this yields no explanation for the observed time behaviour of ice slurries.

The volume V_i of the model particle number i is given by

$$V_i = \frac{\pi}{2} b_i^2 \left(\frac{b_i}{3} + \frac{d_{i\,eff}}{2} \right), \qquad d_{i\,eff} = \frac{1}{f} d_{i\,obs} \tag{2a,b}$$

The effective length d_{ieff} is taken into consideration (corrected with the view factor presented in chapter 3.1). Then the average volume of the whole ensemble with N particles is calculated

$$< V >= \frac{1}{N} \sum_{i=1}^{N} V_i \tag{3}$$

At the boarder of the photograph only the observable fractions of the ice particles are taken into consideration.

The ice fraction is defined by

$$c_I = \frac{m_I}{m} = \frac{N < V > \rho_I}{V \rho} = n < V > \frac{\rho_I}{\rho} \tag{4a-c}$$

The particle density n occurs in equation (4c) and the volume V is defined by the size of the photographic area A_{photo} and the exposure height h

$$n = \frac{N}{V}, \qquad V = A_{photo} h \tag{5a,b}$$

Then it follows that

$$c_I = \frac{< V >}{A_{photo}\ h} \frac{\rho_I}{\rho} N \tag{6}$$

The numerical values are:

- N = 15.3 (microscopy and statistical estimation)
- $\langle V \rangle$ = $1.74 \cdot 10^7$ μm^3 (statistics and model with viewfactor)
- ρ_I = 916.1 kg/m^3 (from chemical handbooks)
- ρ = 967.7 kg/m^3 (measured)
- h = 2000 μm (identical to the distance between the glass plates)
- A_{photo} = 1061 μm x 762 μm. (measured)

With help of equation (6) and these numerical data c_I = 15.6 % is calculated. The physical properties model [15] applied to the same conditions shows a little higher value: c_I = 16.1 %. This model yields results for the density, the enthalpy and the ice fraction. Up to present only the density and the enthalpy function have been confirmed by direct measurements. The good agreement of these two physical properties with experimental data gives support to the assumption that the ice fractions are also correctly predicted. But still it is valuable to have an additional method of direct investigation of the ice fraction. The agreement of results of the two distinct methods is good. But the good result in this single example is a little missleading. It is based on one photograph only, which yields not enough statistical material to obtain a significant result. A fast estimation shows that for other pictures the calculated ice fractions deviate by a few percent. Therefore, in future we intend to evaluate larger statistical data sets to establish the proposed method to directly determine ice fractions.

4.3 Ultrasound Velocity Profile Measurements

In a horizontal pipe with laminar ice slurry flow the downstream velocity component is measured at different locations in the radial direction. The mass flow is 0.5 kg/s.

In the flow on each ice particle two forces act. The ice particles are connected to the carrier fluid by viscous friction and according to the Archimede's law the density difference between the ice and the fluid leads to buoyancy. In these experiments a horizontal profile is measured, which is less affected by buoyancy than a vertical profile. The obtained profiles are symmetric to the axis of the pipe.

From a velocity profile it is possible to construct a complete rheogram, if additionally the pressure drop is measured. Taking the laminar flow theory of a Bingham fluid into consideration (see Ref. [16]), one finds for the critical shear stress

$$\tau_0 = -\frac{1}{2} r_1 \frac{dp}{dz} \tag{7}$$

and for the viscosity

$$\mu = -\frac{1}{4} \frac{1}{u(r_1)} \frac{dp}{dz} (r_2 - r_1)^2 \tag{8}$$

Velocity profiles were thoroughly investigated with the UVP method, but without taking data on the pressure drops. Ben Lakhdar shows experimentally determined rheograms with the same concentration of talin in water [17]. That gives us the possibility to calculate the pressure drop of a pipe of length 1 m, diameter 23 mm, with a mass flow of 0.5 kg/s as adjusted in our experiments. The density was determined to be 967.7 kg/m^3. The result is dp/dz = - 4850 Pa/m. With these data the velocity profiles are calculated (see figure 9).

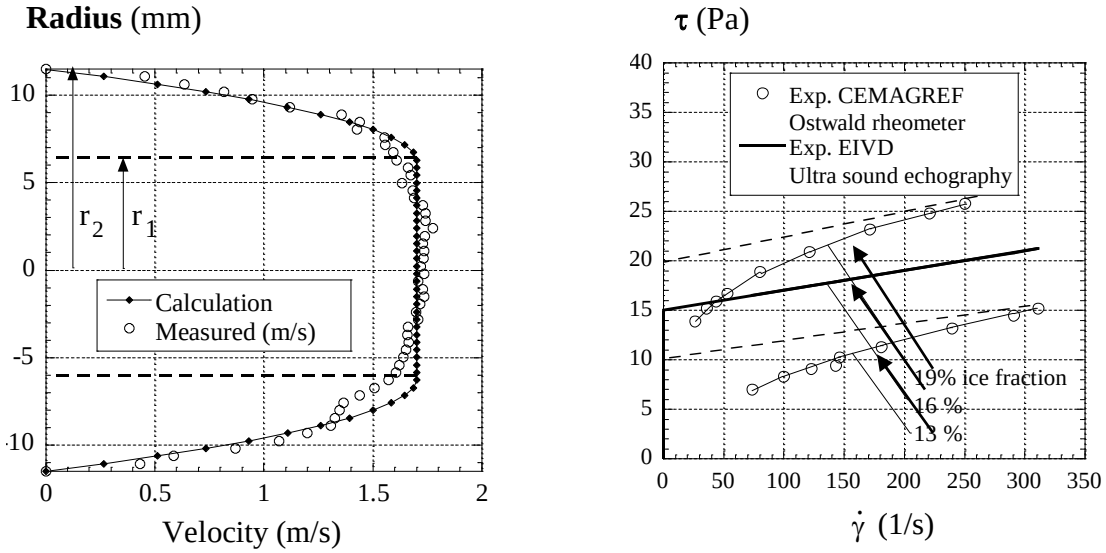

Figure 9: On the left hand side the measured and calculated velocity profiles are compared. On the right rheograms measured with 13% and 19 % ice fractions at CEMAGREF, Paris, France [17] and the idealized rheogram, constructed with the viscosity and critical shear stress determined with the UVP method (data obtained from the figure on the left) are shown.

Because of small disturbances in the measurement of the velocity profile the radius of the rectangular plug r_1 may be difficult to determine. The result can be improved by fitting parabolic curves into the two flanks of the measured profile and afterwards to estimate the positions of the maximas of these two parabolas, which define direct measures of r_1.

5. CONCLUSIONS

A microscopic method to determine the ice fraction is presented, which shows first good results. The ensemble of the statistical evaluation must be chosen a factor ten larger to decide, if the method can yield ice fractions with an inacccuracy of less than 5%. To relate to the geometrical projection, in a simple model consideration a form view factor is calculated. The microscopic pictures taken in two different experiments do not give significant evidence for an alteration of ice particle shape and size as a function of time, which would explain the observed time behaviour.

In Ref. [14] a first vertical velocity profile of ice slurry measured with the UVP method in a horiziontal tube has been presented. Here, a new horizontal profile of laminar flow, also measured in a horizontal tube, is compared with the Bingham theory and combined with rheological quantities measured at CEMAGREF near Paris, France. The results show good agreement.

NOMENCLATURE

Standard

A_{photo}	photographic area	(m^2)
b	width	(m)
c_T	concentration of talin	(-)
c_I	ice fraction	(-)
d	length	(m)
d_{obs}	observed length (in a projection)	(m)
f	view factor	(-)
h	depth of exposure	(m)
I	double integral	(-)
l	length	(m)
l_{eff}	effective length	(m)
m_I	mass of ice particles in slurry	(kg)
m	total mass of ice slurry	(kg)
n	particle density	(m^{-3})
N	number of particles	(-)
$n_{rot\ stock}$	frequency of mixing element	(Hz)
$n_{rot\ prod}$	frequency of scraper in the ice generator	(Hz)
p	pressure	(Pa)
r_1	radius of plug	(m)
r_2	radius of pipe	(m)
T_{evap}	evaporation temperature	(°C)
u,U	velocity	(m/s)
V	volume	(m^3)
z	axial cordinate	(m)

Greek

α	angle	(rad)
$\dot{\gamma}$	shear velocity	(s^{-1})
φ	angle	(rad)
ϑ	temperature	(°C)
μ	viscosity	(Pas)
θ	angle	(rad)
ρ	density	(kg/m^3)
σ	standard deviation	(μm)
τ	shear stress	(Pa)
τ_0	critical shear stress	(Pa)

ACKNOWLEDGEMENTS

We are grateful to R. List for helpful remarks. Ph. Moser, G. Chollet and A. Cavin we thank for technical assistance. The support of the FIFE work by the “Projekt- und Studienfonds der Elektrizitätswirtschaft (PSEL)” and the “Kommission für Technologie und Innovation (KTI)” is gratefully acknowledged.

REFERENCES

[1] Vuarnoz, D., 1999, Visualisation d'un fluide biphasique, *Diploma work at the University of Applied Sciences of Western Switzerland*.

[2] Frei, B., Egolf, P. W., 2000, Viscometry Applied to the Modified Bingham Substance Ice Slurry. *Proceedings of the Second Workshop on Ice Slurries*, Paris, France, 25-26 May (accepted).

[3] Turian, R. M., Yuan, T.-F., 1977, *AIChE Journal* **23** (3), 232-243.

[4] Washington, C., 1993, *Particle Size Analysis in the Pharmaceutics and other Industries*, Ellis Horwood.

[5] Allen, T. 1992, *Particle Size Measurement*, 4 th. Edition, Chapman and Hall, ISBN 0 412 35 070.

[6] Fukusako, S., Kozawa, Y., Yamada, M.,, Tanino, M., 1999, Research and Development Activities on Ice Slurrries Research in Japan, *Proceedings of the First Workshop on Ice Slurries*, Yverdon-les-Bains, Switzerland, 27-28 May, 83-105.

[7] Bel, O., 1996, Contribution à l'Étude du comportement thermo-hydraulique d'un mélange diphasique dans une boucle frigorifique a stockage d'énergie, Ph D thesis, No. 96 ISAL 0088, L' Institute National des Sciences Appliquées de Lyon, France.

[8] Kauffeld, M., Christensen, K. G., Lund S., Hansen, T. M., 1999, *Proceedings of the First Workshop on Ice Slurries*, Yverdon-les-Bains, Switzerland, 27-28 May, 42-73.

[9] Windhab, E., Ouriev, B., Wagner, T., Drost, M., 1996, Rheological Study of Non-Newtonian Fluids, *First Int. Symposium on Ultrasonic Doppler Methods for Fluid Mechanics and Fluid Engineering*, Paul Scherrer Institute, Villigen, Switzerland, 9-11 September.

[10] Mori, M., Takeda, Y., Furuichi, N., 1999, Development of a New Type Flow Metering System using UVP, *First Int. Symposium on Ultrasonic Doppler Methods for Fluid Mechanics and Fluid Engineering*, Paul Scherrer Institute, Villigen, Switzerland, 9-11 September.

[11] Yamanaka, G., Kikura, H., Takeda, Y., Aritomi, M., 1999, Flow Measurement on Oscillating Pipe Flow near the Entry using UVP Method. *First Int. Symposium on Ultrasonic Doppler Methods for Fluid Mechanics and Fluid Engineering*, Paul Scherrer Institute, Villigen, Switzerland, 9-11 September.

[12] Wunderlich, Th., Brunn, P. O., 1990, *Flow Measurement and Instrumentation* **10**, 201-205.

[13] Kawashima, T., Saqsaki, M., Takahashi,, H., 1993, Experimental Studies of Snow-water Mixture Flows in Horizontal Pipes, *Twelfth Int. Conf. on Slurry Handling and Pipeline Transport, Hydrotransport 12*, Mechanical Engineering Publications Limited, London.

[14] Egolf, P. W., Sari, O., Meili, F., Moser, Ph., Vuarnoz, D., 1999, Heat Transfer of Ice Slurries in Pipes, 1999, *Proceedings of the First Workshop on Ice Slurries*, Yverdon-les-Bains, Switzerland, 27-28 May, 106-123.

[15] Egolf, P. W., Frei, B., 1999, The Continuous-properties Model for Melting and Freezing applied to Fine-crystalline Ice Slurries, 1999, *Proceedings of the First Workshop on Ice Slurries*, Yverdon-les-Bains, Switzerland, 27-28 May, 25-40.

[16] Egolf, P. W., Brülmeier, J., Özvegyi, F., Abächerli, F., Renold, P, 1996, *Kältespeicherungseigenschaften und Strömungsverhalten von binärem Eis*, Forschungsbericht zuhanden der Stiftung zur Förderung des Zentralschweizerischen Technikums, Juni.

[17] Lakhdar, M. A .B., 1998, Comportement thermohydraulique d'un fluide frigoporteur diphasique: le coulis de glace, Ph D thesis, L' Institut National des Sciences Appliquées de Lyon, France, April.

[18] Sari, O., Meili, F., Vuarnoz, D., Egolf, P. W., 2000, Thermodynamics of Moving and Melting Ice Slurries, *Proceedings of the Second Workshop on Ice Slurries*, Paris, France, 25-26 May (accepted).
[19] Communication with R. List.